Heterochromatin protein 1 mediates development and aggressiveness of neuroendocrine prostate cancer

Journal Item

Heterochromatin protein 1α mediates development and aggressiveness of neuroendocrine prostate cancer

Authors: Xinpei Ci[1,2], Jun Hao[1,2], Xin Dong[2], Stephen Y. Choi[1,2], Hui Xue[2], Rebecca Wu[2], Sifeng Qu[1,2], Peter W. Gout[2], Fang Zhang[2], Anne M. Haegert[1], Ladan Fazli[1], Francesco Crea[3], Christopher J. Ong[1], Amina Zoubeidi[1], Housheng H. He[4,5], Martin E. Gleave[1], Colin C. Collins[1], Dong Lin[1,2,*], Yuzhuo Wang[1,2,*]

Author affiliation: [1]Vancouver Prostate Centre, Department of Urologic Sciences, University of British Columbia, Vancouver, BC, Canada.

[2]Department of Experimental Therapeutics, BC Cancer, Vancouver, BC, Canada.

[3]School of Life, Health & Chemical Sciences, The Open University, Walton Hall, Milton Keynes, MK7 6AA, United Kingdom.

[4]Princess Margaret Cancer Center, University Health Network, Toronto, Ontario, Canada.

[5]Department of Medical Biophysics, University of Toronto, Toronto, Ontario, Canada.

Running title: Heterochromatin gene signature unveils HP1α mediating NEPC

Key words: Neuroendocrine prostate cancer, HP1α, Transdifferentiation, PDX

Conflict of Interest: The authors have no conflicts of interest to disclose.

Word Count (Main text): 5069

Number of Figures: 6

* **Corresponding author**:

Yuzhuo Wang
Vancouver Prostate Centre
Department of Urologic Sciences, University of British Columbia
2660 Oak Street, Vancouver,
BC V6H 3Z6, Canada
Phone: 604-675-8013, email: ywang@bccrc.ca

26

27 Dong Lin
28 Vancouver Prostate Centre
29 Department of Urologic Sciences, University of British Columbia
30 2660 Oak Street, Vancouver
31 BC V6H3Z6, Canada
32 Phone: 604-675-7013, email: dlin@prostatecentre.com

33

ABSTRACT (230 WORDS)

Neuroendocrine prostate cancer (NEPC) is a lethal subtype of prostate cancer (PCa) arising mostly from adenocarcinoma via NE transdifferentiation following androgen deprivation therapy. Mechanisms contributing to both NEPC development and its aggressiveness remain elusive. In light of the fact that hyperchromatic nuclei are a distinguishing histopathological feature of NEPC, we utilized transcriptomic analyses of our patient-derived xenograft (PDX) models, multiple clinical cohorts, and genetically engineered mouse models to identify 36 heterochromatin-related genes that are significantly enriched in NEPC. Longitudinal analysis using our unique, first-in-field PDX model of adenocarcinoma-to-NEPC transdifferentiation revealed that, among those 36 heterochromatin-related genes, heterochromatin protein 1α (HP1α) expression increased early and steadily during NEPC development and remained elevated in the developed NEPC tumor. Its elevated expression was further confirmed in multiple PDX and clinical NEPC samples. *HP1α* knockdown in the NCI-H660 NEPC cell line inhibited proliferation, ablated colony formation, and induced apoptotic cell death, ultimately leading to tumor growth arrest. Its ectopic expression significantly promoted NE transdifferentiation in adenocarcinoma cells subjected to androgen deprivation treatment. Mechanistically, HP1α reduced expression of androgen receptor (AR) and RE1 silencing transcription factor (REST) and enriched the repressive trimethylated histone H3 at Lys9 (H3K9me3) mark on their respective gene promoters. These observations indicate a novel mechanism underlying NEPC development mediated by abnormally expressed heterochromatin genes, with HP1α as an early functional mediator and a potential therapeutic target for NEPC prevention and management.

Statement of Significance

Heterochromatin proteins play a fundamental role in neuroendocrine prostate cancer, illuminating new therapeutic targets for this aggressive disease.

INTRODUCTION

Neuroendocrine prostate cancer (NEPC) has become a clinical challenge in the management of castration resistant prostate cancer (CRPC). While *de novo* cases are rare, NEPC as a special subtype of CRPC (~10-20%) is thought to occur via NE transdifferentiation of prostate adenocarcinomas in response to androgen deprivation treatment (ADT), resisting dependence on AR signaling as an adaptive response. As next-generation AR pathway inhibitors (ARPI) such as enzalutamide and abiraterone have made substantial improvements in managing CRPC adenocarcinomas in recent years (1), it is expected that the incidence of NEPC will further increase (2). Unfortunately, the overall median survival of NEPC with small cell feature is less than one year, primarily due to its aggressiveness and limited available treatment options (3). As such, a better understanding of the mechanisms underlying NEPC development remains much needed in order to develop more effective therapeutics.

One distinct histopathological feature of NEPC cells is the frequent manifestation of hyperchromatic nuclei with finely dispersed chromatin and inconspicuous nucleoli, a phenomenon known as “salt and pepper” chromatin (3,4). This is in contrast to prostatic adenocarcinoma cells, which tend to have enlarged nuclei with prominent nucleoli (3,4). This special hematoxylin-staining characteristic suggests a distinct NEPC heterochromatin pattern (5). Heterochromatin is a condensed and transcriptionally inert chromosome conformation, regulated epigenetically by precise and dedicated machineries (6,7). Multiple studies have demonstrated that epigenetic regulation is one major mechanism underlying

NEPC development (8-11). An NEPC-specific heterochromatin gene signature can thus shed light to help better understand the disease and identify novel therapeutic targets. Another distinct feature of NEPC is the lineage alteration associated with a decrease or loss of crucial adenocarcinoma lineage-specific transcription factors, AR, FOXA1 and REST (12-15). This leads to the repression of AR-regulated genes (e.g. prostate-specific antigen (PSA)) and gain of neuroendocrine markers (e.g. neural cell adhesion molecule 1 (NCAM1/CD56), neuronal-specific enolase (NSE), chromogranin A (CHGA), and synaptophysin (SYP)) (12-14). While recent studies have reported that EZH2 inhibits *AR* expression and SRRM4 mediates *REST* splicing (8,16), the mechanisms underlying the constant transcriptional suppression of *AR* and *REST* are still not well understood.

One of the major hurdles in studying NEPC is the lack of clinically relevant models, but substantial progress has been achieved recently in modeling NEPC development. Employing genetically engineered mouse (GEM) models, ectopic gain of *N-myc* and concomitant loss of *Rb1* and *Tp53* have both been demonstrated to induce *de novo* NEPC-like tumors (8,11). Potent ADT using abiraterone in *Tp53*/*Pten* double deficient mice also promoted overt NE transdifferentiation of luminal adenocarcinoma cells (17). Employing engineered human primary cells or cell lines, *N-myc*, *SOX2*, *BRN2*, and *SRRM4* overexpression have all been shown to promote NE transdifferentiation (16,18-20). Our laboratory has established over 45 high-fidelity patient-derived xenograft (PDX) models of PCa including 5 NEPCs (www.livingtumorlab.ca) (21). Among them, LTL331/331R is the first-in-field and unique PDX model of adenocarcinoma-to-NEPC transdifferentiation. Upon host castration, the primary adenocarcinoma (LTL331) initially regresses but relapses within few

102 months as typical NEPC (LTL331R) (21). Importantly, the whole transdifferentiation process
103 observed in the LTL331/331R model is predictive of disease progression and is fully
104 recapitulated in the donor patient (22), suggesting a strong clinical relevance. Because an
105 overwhelming majority of expressed genes accounting for the NE phenotype in terminal
106 NEPC may obscure the real drivers of disease progression required at earlier stages, we
107 focused on identifying the early changes induced by ADT before NEPC is fully developed,
108 with an additional secondary criterion that these changes persist into terminal NEPC. To this
109 end, we developed a time series of the LTL331 model, for which samples were harvested at
110 multiple points during the transition period following host castration in order to monitor the
111 entire transdifferentiation process and discover potential drivers with early expression
112 changes (22).

113 In this study, we identified a heterochromatin molecular signature that is commonly
114 upregulated in NEPC. Among the signature genes, we discovered that the upregulation of
115 HP1α (encoded by *CBX5*), a gene prominently associated with constitutive heterochromatin
116 and mediating concomitant gene silencing, was an early event in our LTL331/331R NE
117 transdifferentiation model. HP1α expression was increased within weeks following castration
118 but before emergence of NE genes, gradually reaching its highest level in terminally
119 developed NEPC. HP1α is also widely expressed in clinical samples of NEPC. We show that
120 HP1α is essential for NEPC cell proliferation, survival, and tumor growth, and its elevated
121 expression promotes ADT-driven NE-differentiation in prostatic adenocarcinoma cells. *HP1α*
122 ectopic expression reduces expression of AR and REST, two crucial transcription factors

123 silenced in NEPC, and enriches the repressive histone mark H3K9me3 on their respective

124 gene promoters.

MATERIAL AND METHODS

Patient-derived xenografts and clinical datasets

All PDX tumor lines were grafted in NSG mice as previously described (21). This study followed the ethical guidelines stated in Declaration of Helsinki, specimens were obtained from patients with their informed written consent form following a protocol (#H09-01628) approved by the Institutional Review Board of the University of British Columbia (UBC). Animal studies under the protocol # A17-0165 were approved by UBC Animal Care and Use Committee. The LTL331 castrated tissues and the NEPC-relapsed LTL331R tissues were harvested at different time points after host castration (22). Transcriptomic analysis for all PDX tumors, with the exception of the LTL331-331R castration time-series samples, was performed using GE 8x60K microarray, as previously described (21). Transcriptomic analysis of the LTL331-331R time-series was done using RNA-sequencing data.

The clinical cohorts used in this study are as follows: RNA-seq data for the *Beltran* et al. 2011 cohort (30 adenocarcinomas, 6 NEPCs) was from Weill Medical College of Cornell University (23); RNA-Seq data for the *Beltran et al*. 2016 (34 CRPC-adenocarcinomas, 15 NEPCs) the *Grasso et al*. 2012 (31 CRPC-adenocarcinomas, 4 NEPCs), and the *Kumar et al*. 2016 (149 CRPC-adenocarcinomas) cohorts were accessed through the cBioPortal (10,24-26); microarray data for the *Varambally et al*. 2015 cohort (6 CRPC-adenocarcinomas) was accessed from the Gene Expression Omnibus (GEO) database (GSE3325) (27).

146

147 **Human prostate cancer specimens**

148 PCa specimens were obtained from the Vancouver Prostate Centre Tissue Bank
149 (103 hormone naive primary prostatic adenocarcinomas, 120 CRPC-adenocarcinomas, 8
150 NEPCs). This study followed the ethical guidelines stated in Declaration of Helsinki,
151 specimens were obtained from patients with their informed written consent form following a
152 protocol (#H09-01628) approved by the Institutional Review Board of the University of British
153 Columbia (UBC). Tissue microarrays of duplicate 1 mm cores were constructed manually
154 (Beecher Instruments, MD, USA). NEPC specimens are histologically either small cell
155 carcinoma or large cell neuroendocrine carcinoma with low or negative AR expression and
156 positive CHGA expression as determined by IHC staining.

157

158 **Cell line culture and reagents**

159 NCI-H660 and 293T cells were obtained from ATCC. Cells were authenticated with
160 fingerprinting method at Fred Hutchinson Cancer Research Centre (Seattle, USA).
161 Mycoplasma testing was routinely performed at the Vancouver Prostate Centre. NCI-H660
162 cells was cultured in RPMI-1640 medium (Hyclone) with supplements as follows: 5% FBS
163 (GIBCO), 10 nM beta-estradiol (Sigma), 10 nM Hydrocortisone (Sigma), 1% Insulin-
164 Transferrin-Selenium (Thermo Fisher). V16D (20) cells were maintained in RPMI-1640
165 containing 10% FBS. 293T was kept in DMEM (Hyclone) with 5% FBS. For *in vitro* NE

phenotype induction in V16D cells, cells were starved with phenol-red free RPMI-1640 (GIBCO) containing 10% Charcoal-Stripped Serum (CSS) (GIBCO) for 24 hours, then cultured in the same media or with the addition of 10 μM enzalutamide (Haoyuan Chemexpress) for another 14 days (20).

Bioinformatics analysis

As previously described, Gene Set Enrichment Analysis (GSEA) (http://software.broadinstitute.org/gsea/index.jsp) was used in this study to determine whether a defined set of genes show significant, concordant differences between two biological phenotypes (e.g. PCa adenocarcinoma vs. NEPC) or two sample groups (e.g. shC vs. KD) (28). All GSEA analyses in this study used whole transcriptomic data without expression level cut-off as expression datasets. Normalized values were used for profiling data from PDX tissues, H660 and V16D stable cell lines, and the three NEPC mouse models (GSE90891, GSE92721, GSE86532); raw read numbers was used for RNA-seq data from the *Beltran et al*. 2011 cohort; pre-ranked gene list based on *p*-value from lowest to highest was used for the *Beltran et al.* 2016 cohort (8,10,11,17,21,23). Unbiased analysis was performed using the latest MSigDB database for each collection (29). Phenotype permutation was applied when the sample size grouped in one phenotype was more than five. Otherwise, gene set permutation was employed. False discovery rate (FDR) q values were calculated using 1000 permutations, a geneset was considered significantly enriched if its normalized enrichment score (NES) has an FDR q below 0.25.

Ingenuity pathway analysis (IPA) was performed as previously described (20). Differentially expressed genes were selected based on the criteria that their standard deviation between samples of one group (e.g. three HP1α knockdown lines) is below 0.5 and their student's *t*-test *p*-value between groups (e.g. shC vs. KD) is below 0.05.

For the NE scores and the heterochromatin score, the weight for each gene in the score list was first calculated by taking the log2 of the *p*-value of all genes and multiplying it by the sign of the fold change. The weight for each gene in *Lee et al*. 2016 was obtained directly from their study. The *p*-values for the genes contributing to heterochromatin score was calculated by comparing NEPC PDXs with all other adenocarcinoma PDXs with the Student's *t*-test. A score was then assigned to each sample by multiplying the weight with the normalized RNA expression value, adding all values for each gene, log-transforming the absolute value of the sum value, and multiplying the sign of the sum value (10,11,18).

The heatmap was constructed using the Gplots and heatmap.2 packages in R. Hierarchal clustering was used to determine sample similarity.

Statistical analysis and data representation

Statistical analysis was done using the Graphpad Prism software. The Student's *t*-test was used to analyze statistical significance between groups in discrete measurements while two-way ANOVA was used for continuous measurements. The Kaplan-Meier method was used to estimate curves for relapse-free survival, and comparisons were made using

the log-rank test. Pearson correlation (with 95% confidence intervals) was used to measure the linear correlation between two variables. Any differences with *p*-values lower than 0.05 is regarded as statistically significant, with *$p<0.05$, **$p<0.01$, ***$p<0.001$. Graphs show pooled data with error bars representing standard error of the mean (SEM) obtained from at least three replicates and standard deviation (SD) of values from clinical samples. Lines in scatter plots represent the median value of measurements from multiple samples and mean with 95% confidence interval (CI) for scores from multiple samples. Box plot with whiskers showing 5-95% percentile values was used to represent analysis of IHC scores.

Accession numbers

All PDX microarray profiles are available at www.livingtumorlab.ca, and accessible under the accession number GSE41193 in the GEO database. RNA-seq profiles for the LTL331/331R castration time-series have been deposited to the European Nucleotide Archive and are available under the accession number ENA: PRJEB9660. Microarray profiles for cell lines are deposited (GSE105033).

RESULTS

NEPC has a distinctive heterochromatin gene signature

To determine if a specific gene expression program contributes to the hyperchromatic histological feature of NEPC cells, we first performed an unbiased gene set enrichment analysis (GSEA) using our latest PDX collection and two NEPC clinical cohorts. Transcriptomic profiles from our high-fidelity PDX models (18 adenocarcinomas vs. 4 NEPCs), the *Beltran*, et al. 2011 cohort (30 adenocarcinomas vs. 6 NEPCs), and the *Beltran*, et al. 2016 cohort (34 CRPC-adenocarcinomas vs. 15 NEPCs) (10,21,23) all demonstrate that heterochromatin-associated genes are significantly enriched in NEPC compared to adenocarcinoma (Fig. 1A-1C, S1A). We further analyzed three GEM models mimicking the development of NEPC. Interestingly, heterochromatin-associated genes are also significantly enriched as long as NE differentiation occurs, driven by either *Pten/Rb* double knockout (DKO) or *Pten/Rb/Tp53* triple knockout (TKO), *Pten/Tp53* knockout with potent ADT, or *N-Myc* overexpression (Fig. 1D-1F) (8,11,17).

To further decipher the genes contributing to the heterochromatin feature of NEPC, we analyzed the leading edge genes derived from the GSEA of PDX and clinical NEPC samples (Fig. 1A-1C). Since the NEPCs in our PDX collection are all typical neuroendocrine carcinomas without mixed adenocarcinoma tissues, the upregulated genes identified in the NEPC PDXs and validated in the clinical cohorts can be considered heterochromatin signature genes. In addition, three polycomb-group (PcG) genes, *EZH2*, *RBBP4* and *RBBP7*, are also included in this gene signature as their upregulated expression in NEPC have been

previously reported (9,23). They have also been reported to play important roles in heterochromatin formation (7), but are omitted from the GSEA geneset (GO:0000792) containing other PcG members. As such, 36 genes were identified and selected to form a heterochromatin gene panel, which could successfully distinguish NEPC from adenocarcinoma through hierarchical clustering similar to two reported NE score gene panels (Fig. 1G, S1B-S1E) (10,18). From this heterochromatin gene panel, a weighted score was calculated for each sample in the PDX and clinical cohorts following a similar strategy utilized in recent studies (10,11,18). Notably, similar to NEPC samples having a distinctly higher NE score compared to adenocarcinomas, NEPC samples also have a significantly higher heterochromatin score compared to adenocarcinoma (Fig. 1H). Importantly, the heterogeneity among PDX samples is much smaller than that observed in any clinical cohorts regardless of the scoring system employed, further demonstrating that our PDX collection both clearly reflects the clinical features of NEPC and adenocarcinoma and provide a distinct system to study PCa subtypes. Together, these analyses indicate that a heterochromatin-related gene expression signature is a unique feature of NEPC tumors.

Expression of heterochromatin protein 1α (HP1α) is upregulated early and steadily during NEPC development

Inspired by the critical functional role of heterochromatin structure in modulating cell behavior and gene expression (6,7), we hypothesized that these NEPC-specific heterochromatin signature genes could contribute to NEPC development. As such, we

attempted to identify a potential NEPC driver gene from our 36 heterochromatin signature genes. In addition to a final upregulation in terminal NEPC, expression of the candidate driver gene would also be increased early prior to full NEPC development. We thus analyzed the RNA-seq profile of the LTL331/331R NE-transdifferentiation model with samples from castration-induced dormant time points prior to full NEPC relapse (21,22). Ranked by the gene expression difference between pre- and post-castration samples, elevated expression of *HP1α* was found to be an early and dramatic event occurring upon host castration. Conversely, expression of other genes that have been reported to be associated with NEPC such as *EZH2* and *CBX2* (9,23) were only upregulated in the fully developed NEPC sample (LTL331R) (Fig. 2A). Interestingly, we also noticed that *Hp1α* expression gradually increased as the NE phenotype progressed from partial to more dominantly overt in the *Pten/Tp53* CRPC mouse model (Fig. S2A), lending further support that elevated *HP1α* expression is an early event in NEPC development.

To validate our findings, we performed quantitative RT-PCR (qRT-PCR) to detect *HP1α* expression at the mRNA level and IHC staining and Western blotting to detect HP1α expression at the protein level in our PDX collection. Both the mRNA and protein levels of HP1α are significantly increased in NEPC PDXs (Fig. 2B-2D, S2B). Furthermore, we confirmed HP1α expression in the LTL331/331R castration time-series samples. Consistent with the RNA-seq data, both the mRNA and protein expression of HP1α increased upon host castration, with increased mRNA observed as early as 1 week post-castration and elevated protein expression observed 3 weeks post-castration (Fig. 2E-2G). Taken together, these

data demonstrate that elevated expression of HP1α is an early and consistent event throughout NEPC development and could be a potential driver of NEPC.

HP1α expression is upregulated in clinical NEPC samples and correlates with poor prognosis

To determine the clinical relevance of elevated HP1α expression in NEPC, we analyzed RNA expression profiles from three individual clinical cohorts containing NEPC samples. In the *Beltran* et al. 2011 cohort, *HP1α* expression was about 4 times higher in NEPCs (n=6) compared to adenocarcinomas (n=30) (Fig. 3A) (23). In the *Beltran* et al. 2016 cohort, *HP1α* expression was also significantly upregulated in NEPCs (n=15) compared to CRPC adenocarcinoma samples (n=34) by around two folds (Fig. 3B) (10). In another cohort consisting of 35 metastatic CRPC samples, 4 samples with NEPC features expressed significantly higher *HP1α* mRNA than other typical adenocarcinomas (Fig. 3C) (24). To better understand the relationship between HP1α expression and the NEPC phenotype at a protein level, we performed IHC for HP1α with the Vancouver Prostate Centre (VPC) clinical PCa tissue microarrays (TMAs) containing 103 primary adenocarcinomas, 120 CRPC adenocarcinomas and 8 typical NEPC samples. Consistent with its mRNA level, HP1α protein was significantly overexpressed in NEPCs (mean=2.45) compared to primary adenocarcinomas (mean=1.66, p=0.011) and CRPC adenocarcinomas (mean=1.60, p=0.014) (Fig. 3D, 3E). These data together demonstrate that HP1α is highly expressed in NEPC.

While HP1α is dramatically upregulated in NEPC, we also noticed that some adenocarcinomas also expressed higher levels of HP1α than others (Fig. 3D). We then investigated whether the expression of HP1α is associated with poor patient prognosis, thus possibly being a pre-disposing factor to poor outcome. Among the 103 primary adenocarcinoma samples in the VPC cohort, there were 37 samples with clinical follow-up information. Kaplan-Meier analysis showed that patients with high expression of HP1α (IHC score>=2) had a significantly shorter disease-free survival time (HR=4.627, p=0.0074) than low HP1α-expressing patients (IHC score <2) (Fig. 3F). For CRPC patients, the group with high expression of *HP1α* (top 1/3) had a significantly shorter overall survival time after the first hormonal therapy (HR=2.961, p=0.021), implying that HP1α positively correlates with poor prognosis upon hormonal therapy (Fig. 3G). Overall, these analyses indicate that increased expression of HP1α is a poor prognostic factor in advanced PCa.

***HP1α* knockdown inhibits NEPC cell proliferation and induces apoptosis, leading to tumor growth arrest**

Considering that HP1α is significantly upregulated in NEPC, we proceeded to investigate its function in NEPC cells. NCI-H660 is a unique and typical NEPC cell line (30). Consistent with the high HP1α expression observed in clinical NEPC samples, HP1α is also expressed at the highest level in H660 cells compared to seven other PCa cell lines at both RNA and protein levels (Fig. S3A). We thus constructed stable H660 cell lines with *HP1α* knocked down using lentiviral-delivered shRNAs (Fig. 4A). Upon *HP1α* knockdown, the

overall proliferation of H660 cells was significantly inhibited, as evaluated by both crystal violet staining and cell counting (Fig. 4B, S3B). We further performed colony formation assays to evaluate the reproductive and survival ability of single cells. Remarkably, *HP1α* knockdown was able to ablate the colony formation ability of H660 cells (Fig. 4C). We then proceeded to analyze in greater detail the potential cellular mechanisms underlying the attenuation of cell growth mediated by *HP1α* knockdown. An EdU incorporation assay showed that knockdown of *HP1α* led to a significant reduction of EdU-positive, DNA synthesis-active cells (Fig. 4D). Furthermore, an apoptosis assay and FACS analysis indicated that *HP1α* knockdown also promoted cell early-apoptosis and final death (Fig. 4E, 4F). Molecularly, the apoptosis markers cleaved-caspase 3 and cleaved-PARP1 were both upregulated in knockdown cells (Fig. 4G); multiple machineries involved in DNA damage repair and cell cycle progression were also impaired in *HP1α* knockdown cells as determined by GSEA and ingenuity pathway analysis (IPA) from stable cell line transcriptomic profiles (Fig. 4H, S3C, S3D). Thus, *HP1α* depletion inhibited NEPC cell proliferation and induced apoptosis *in vitro*.

We then assessed the functional impact of *HP1α* knockdown on tumor growth *in vivo*. Compared to control H660 cells, xenograft tumor growth of the KD2 stable cell line with 70% *HP1α* knockdown (Fig. 4A, S3E) was observed to be dramatically inhibited and much slower, as determined by continuous tumor volume measurements and final fresh tumor weights (Fig. 4I, 4J). The other two stable lines (KD1, KD3) with 80%~95% *HP1α* knockdown were not able to generate sufficient cell numbers for *in vivo* tumor formation assays. Taken

348 together, the *in vitro* and *in vivo* studies establish that *HP1α* knockdown could both inhibit
349 NEPC cell proliferation and induce apoptosis, leading to NEPC tumor growth arrest.

350

351 **HP1α promotes NE transdifferentiation of prostatic adenocarcinoma cells following**
352 **ADT**

353 Since HP1α was identified as a potential early driver of NEPC development following
354 hormone therapy, we further investigated whether HP1α could enhance NE phenotype in
355 ADT-induced NE differentiation of adenocarcinoma cells similar to our LTL331/331R NE-
356 transdifferentation PDX model. We used V16D cells, a LNCaP-derived CRPC cell line (20),
357 to construct stable cell lines with *HP1α* ectopic expression (Fig. 5A). Upon ADT using
358 charcoal-stripped serum (CSS) or enzalutamide (EnZ) treatment for 14 days, both control
359 and *HP1α*-overexpressing V16D cells were assessed for the expression of terminal NE
360 markers. *HP1α* overexpression significantly promoted the expression of NCAM1 (CD56) and
361 NSE, as shown by both qRT-PCR and Western blotting (Fig. 5B, 5C). *HP1α* overexpression
362 alone was not able to induce NE transdifferentiation (Fig. 5B, 5C). Further transcriptomic
363 analysis of control and *HP1α*-overexpressing V16D cells upon EnZ treatment revealed that
364 *HP1α* overexpression consistently upregulated the expression of a panel of NEPC marker
365 genes and enriched neuronal-associated signaling pathways (Fig. 5D, 5E, S4A). Pearson
366 correlation analyses with transcriptomic data from multiple CRPC clinical cohorts (i.e., the
367 *Beltran et al.* 2016, the *Kumar et al.* 2016, the *Grasso* et al. 2012, and the *Varabally* et al.
368 2005) further demonstrated that high expression of *HP1α* is positively correlated with the

expression of terminal NE markers (i.e., *NCAM1, NSE, CHGA, CHGB*) in advanced PCa (10,24,25,27) (Fig. 5F, 5G, S4B, S4C). Overall, these analyses suggest that HP1α is a potential functional driver promoting NE transdifferentiation.

HP1α represses AR and REST expression and enriches H3K9me3 on their promoters

We further analyzed how HP1α contributed to the NE phenotype. A major function of HP1α in heterochromatin is to repress gene expression using epigenetic machineries (31,32), which is an observation supported by our transcriptomic analyses with *HP1α* knockdown and overexpressing cells (Fig. 5E, S4D). Decreased or loss of expression of the crucial adenocarcinoma lineage-specific transcription factors AR, FOXA1 and REST is a well-established mechanism leading to NE differentiation (12-14). Notably, when *HP1α* was overexpressed in V16D cells, AR and REST were downregulated at both the mRNA and protein levels (Fig. 6A, 6B, S5A). Consistently, a panel of AR target genes that are repressed in clinical NEPCs are also downregulated upon *HP1α* overexpression in V16D cells (Fig. 6C). Reciprocally, *HP1α* knockdown in H660 cells reactivated *AR* and *REST* mRNA expression (Fig. S5B), though their protein levels remained undetectable due to low abundance.

We next investigated potential mechanisms underlying the downregulation of AR and REST upon *HP1α* overexpression. We found that, rather than affecting global heterochromatin related genes, *HP1α* overexpression significantly enriched (while knockdown impaired) pericentric heterochromatin machineries as determined by GSEA

(Fig.6D, S5C-S5E). Pericentric heterochromatin is a constitutive heterochromatin structure characterized by the repressive histone mark H3K9me3 (32). We then performed a chromatin immunoprecipitation (ChIP) assay to examine the occupancy of H3K9me3 on the promoter regions of *AR* and *REST* following *HP1α* modulation. Interestingly, in V16D cells, *HP1α* overexpression increased the occupancy of H3K9me3 on both the *AR* and *REST* promoters, while its knockdown in H660 cells decreased H3K9me3 enrichment on the *AR* promoter (Fig. 6E, S5F). In accordance with our findings in cell lines, the pericentric heterochromatin geneset is consistently and significantly enriched in NEPCs compared to adenocarcinomas in our PDX models, multiple clinical cohorts, and GEM models (Fig. 6F, S5G). Meanwhile, Pearson correlation analyses with multiple clinical cohorts showed that *HP1α* expression is negatively correlated with *AR* and *REST* expression in advanced PCa samples (Fig. 6G, 6H, S5H) (10,24,25,27). Overall, our data indicate that HP1α could regulate expression of the two crucial adenocarcinoma lineage-specific transcription factors AR and REST potentially via modulating the enrichment of H3K9me3 on their promoters.

DISCUSSION

Loss of luminal epithelial cell characteristics together with gain of small cell neuroendocrine features makes NEPC a completely different disease than typical adenocarcinoma CRPC. This transdifferentiation makes all ARPIs inapplicable despite their otherwise remarkable revolution on the treatment of advanced PCas (1,14). More critically, the application of potent ARPIs for the clinical management of CRPC could accelerate the incidence of NEPC in near future (2,3,33). As such, deciphering the biological and molecular mechanisms underlying NEPC development is fundamentally important for developing novel therapeutics.

Gross differences in nuclear hyperchromatic morphology between adenocarcinoma cells and NEPC cells have long been a criterion for NEPC pathological diagnosis. Our study here unmasks, for the first time, the precise molecular basis underlying this NEPC-specific nuclear phenotype and identifies a 36-gene NEPC heterochromatin signature using multiple high-fidelity prostatic adenocarcinoma and NEPC PDXs and two prevalent clinical cohorts. Notably, our heterochromatin gene signature can significantly distinguish NEPCs from adenocarcinomas similar to two other NEPC gene signatures derived from whole-genomic differences, suggesting a crucial function of heterochromatin in NEPC and also a potential application for diagnostic purposes. Furthermore, as epigenetic machineries play a major foundational role in heterochromatin formation and function (6,34), this 36-gene heterochromatin signature also includes 29 epigenetic factors (35). Among them, PcG genes such as *EZH2* have already been demonstrated to play critical roles in NEPC (8,9,36). Thus,

these heterochromatin genes also provide a molecular basis for NEPC development and aggressiveness. Considering that the hyperchromatic nuclear pattern in NEPC is also shared by other small cell carcinomas such as small cell lung cancer (SCLC), this heterochromatin signature may be further applicable to small cell carcinomas of other tissue origins (37).

From these 36 heterochromatin genes, HP1α was identified as a potential early driver of NE transdifferentiation. The longitudinal analyses of LTL331 PDX tissues following host castration demonstrated that the upregulated expression of HP1α is an early event. This is in contrast to a number of genes previously reported to be involved in NEPC development, such as *EZH2*, *CBX2* (9,23), which were only upregulated in the fully developed NEPC LTL331R tumor. Notably, our LTL331/331R model is not only clinically relevant (21,22), but also highly reproducible in delivering the same NE transdifferentiation in 18 individual repeats without exception so long as castration is applied. This robust phenomenon indicates that NE transdifferentiation in the LTL331/331R model is lineage determined, and the early changes detected in castrated tumors may thus reflect an inevitable and not stochastic event. More importantly, we indeed demonstrate that HP1α can promote terminal NE marker expression in adenocarcinoma cells following ADT. In our study, we also noticed that while HP1α was able to repress AR expression and AR signaling under AR-driven prostatic epithelial status, it cannot function as a neural factors to directly induce the NE phenotype. Only when AR signaling is diminished by ADT can *HP1α* ectopic expression promote NE transdifferentiation in adenocarcinoma cells. This process both recapitulates the *in vivo* NE transdifferentiation phenotype occurring in the LTL331/331R

model, and also mirrors the clinical progression of NEPC where most cases appear after hormonal therapy (3,33). In terminal NEPC cells where HP1α mainly functions as a regulator of aggressiveness, *HP1α* knockdown cannot alter NE phenotype (Fig. S6A). Therefore, HP1α could potentially serve as an early therapeutic target to interfere with disease progression before NEPC fully develops.

In addition to being significantly overexpressed in clinical NEPC samples, HP1α plays a crucial role in terminal NEPC as demonstrated by thorough functional studies in the *bona fide* NEPC cell line NCI-H660. While previous studies have reported the function of HP1α in breast cancer, lung cancer, and cholangiocarcinoma, its function in prostate cancer remains elusive (38-42). Our data demonstrates that *HP1α* knockdown in NEPC cells dramatically inhibited proliferation, completely ablated colony formation, and induced apoptotic cell death. Consequently, *HP1α* depletion markedly inhibited NEPC tumor growth *in vivo*. Alternatively, in V16D adenocarcinoma cells where *HP1α* overexpression promoted NE transdifferentiation, *HP1α* overexpression did not significantly enhance proliferation (Fig. S6B). These data suggests that HP1α is particularly essential for NEPC malignancy, with one potential mechanism being *HP1α* depletion impairs mitotic machineries. While reported to drive and maintain heterochromatin structure (31,32,43), HP1α is prominently associated with constitutive heterochromatins (44) as demonstrated through our study. Depletion of *HP1α* did not affect heterochromatin-related genes universally, but significantly impaired the pericentric constitutive heterochromatin machineries. Pericentric heterochromatin is a key element ensuring proper chromosome segregation in metaphase (6), which is also a major previously reported function of HP1α (38,45). The abnormally enriched pericentric

469 heterochromatin genes in NEPCs may also explain the highly proliferative feature of NEPC,
470 for which HP1α may play a driver function. Another potential mechanism underlying the
471 essential function of HP1α in NEPC aggressiveness is that *HP1α* depletion impaired DNA
472 damage response (DDR) machineries, which is in accordance with previous studies (46,47).
473 Most recently, another study also reported that a DDR pathway is enriched in NEPC,
474 contributing to NEPC cell proliferation (48). Overall, HP1α could potentially serve as a
475 therapeutic target for effective management of developed NEPC.

476 Our findings also suggest a novel, HP1α-mediated mechanism of NEPC
477 development. AR, FOXA1 and REST are the three crucial adenocarcinoma lineage-specific
478 transcription factors maintaining luminal epithelial characteristics (12-14). Our data
479 demonstrates that HP1α can repress AR and REST expression in adenocarcinoma cells,
480 while its depletion in NEPC cell can reactivate their expression. *HP1α* gene was first
481 identified to be a modulator of position effect variegation where euchromatic genes
482 abnormally juxtaposed with pericentric heterochromatin could be silenced due to compaction
483 into heterochromatin (49). In our study, we also found that HP1α may play an epistatic role
484 in regulating the pericentric heterochromatin apparatus. The repressive histone mark
485 H3K9me3 is a hallmark of pericentric heterochromatin and also a major substrate
486 recognized by HP1α (31,32). Given that the *AR* and *REST* genes are natively located in the
487 vicinity of pericentric heterochromatins (Xq12 and 4q12 respectively, Fig. S6C), they could
488 potentially be sensitive to pericentric heterochromatin deregulation. Our data indeed showed
489 that modulation of *HP1α* regulates the enrichment of H3K9me3 on the promoters of *AR* and
490 *REST*. Considering the significant enrichment of H3K9me3-characterized pericentric

heterochromatin genes in multiple NEPC models and clinical cohorts, our study suggests that the HP1α/H3K9me3 axis may partially explain the absence or loss of AR and REST expression in NEPCs. Further investigation on genome-wide occupancy of HP1α and H3K9me3 will provide valuable insights. HP1α mediates gene silencing together with other precise epigenetic machineries (31). Previous studies have shown that *AR* expression can also be repressed by the EZH2/H3K27me3 axis (8,36). As such, HP1α/H3K9me3 might coordinate with EZH2/H3K27me3, establishing the complete repression of *AR* in NEPCs. Alternative splicing has been suggested to suppress REST in NEPCs (16). HP1α was also reported to mediate mRNA alternative splicing and exon recognition (50). As such, HP1α might be involved in mediating *REST* splicing as well. Our data here suggests HP1α/H3K9me3 as a new mechanism leading to the silencing of *REST* mRNA in most NEPC samples.

In summary, our data imply a novel mechanism underlying NEPC development: HP1α drives the abnormal formation of pericentric heterochromatin, which in turn promotes ADT-induced NE transdifferentiation via repressing AR and REST expression, and confers the malignant NEPC phenotype via promoting aggressive proliferation and cell survival. Taken together HP1α can be considered an early and master mediator of NEPC development and aggressiveness, making it an exceptional novel therapeutic target for potentially effective treatment of NEPC.

ACKNOWLEDGEMENTS

We would like to thank all members of Y.Z.Wang laboratory for technical support and helpful discussions. We also would like to thank Dr. Jin-Tang Dong (Emory University, USA) for providing the plasmids described herein. This work was supported in part by the Canadian Institutes of Health Research (Y.Z.Wang), Terry Fox Research Institute (Y.Z.Wang, ME. Gleave, C.Collins, C.Ong), BC Cancer Foundation (Y.Z.Wang), Urology Foundation (Y.Z.Wang), and Prostate Cancer Canada (Y.Z.Wang). X.Ci was supported by Prostate Cancer Canada-Movember training award. J.Hao and S.Qu were supported by Mitacs Accelerate award. S.Choi was supported by the CIHR Doctoral award.

REFERENCES

1. Attard G, Parker C, Eeles RA, Schroder F, Tomlins SA, Tannock I*, et al.* Prostate cancer. Lancet **2016**;387(10013):70-82 doi 10.1016/S0140-6736(14)61947-4.
2. Eric Jay S, Rahul Raj A, Jiaoti H, Artem S, Li Z, Joshi JA*, et al.* Clinical and genomic characterization of metastatic small cell/neuroendocrine prostate cancer (SCNC) and intermediate atypical prostate cancer (IAC): Results from the SU2C/PCF/AACRWest Coast Prostate Cancer Dream Team (WCDT). Journal of Clinical Oncology **2016**;34(15_suppl):5019- doi 10.1200/JCO.2016.34.15_suppl.5019 %U http://ascopubs.org/doi/abs/10.1200/JCO.2016.34.15_suppl.5019.
3. Vlachostergios PJ, Puca L, Beltran H. Emerging Variants of Castration-Resistant Prostate Cancer. Curr Oncol Rep **2017**;19(5):32 doi 10.1007/s11912-017-0593-6.
4. Humphrey PA. Diagnosis of adenocarcinoma in prostate needle biopsy tissue. J Clin Pathol **2007**;60(1):35-42 doi 10.1136/jcp.2005.036442.
5. Fischer AH, Jacobson KA, Rose J, Zeller R. Hematoxylin and eosin staining of tissue and cell sections. CSH Protoc **2008**;2008:pdb prot4986 doi 10.1101/pdb.prot4986.
6. Saksouk N, Simboeck E, Dejardin J. Constitutive heterochromatin formation and transcription in mammals. Epigenetics Chromatin **2015**;8:3 doi 10.1186/1756-8935-8-3.
7. Morgan MA, Shilatifard A. Chromatin signatures of cancer. Genes Dev **2015**;29(3):238-49 doi 10.1101/gad.255182.114.
8. Dardenne E, Beltran H, Benelli M, Gayvert K, Berger A, Puca L*, et al.* N-Myc Induces an EZH2-Mediated Transcriptional Program Driving Neuroendocrine Prostate Cancer. Cancer Cell **2016**;30(4):563-77 doi 10.1016/j.ccell.2016.09.005.
9. Clermont PL, Lin D, Crea F, Wu R, Xue H, Wang Y*, et al.* Polycomb-mediated silencing in neuroendocrine prostate cancer. Clinical epigenetics **2015**;7(1):40 doi 10.1186/s13148-015-0074-4.
10. Beltran H, Prandi D, Mosquera JM, Benelli M, Puca L, Cyrta J*, et al.* Divergent clonal evolution of castration-resistant neuroendocrine prostate cancer. Nat Med **2016** doi 10.1038/nm.4045.
11. Ku SY, Rosario S, Wang Y, Mu P, Seshadri M, Goodrich ZW*, et al.* Rb1 and Trp53 cooperate to suppress prostate cancer lineage plasticity, metastasis, and antiandrogen resistance. Science **2017**;355(6320):78-83 doi 10.1126/science.aah4199.
12. Wright ME, Tsai MJ, Aebersold R. Androgen receptor represses the neuroendocrine transdifferentiation process in prostate cancer cells. Mol Endocrinol **2003**;17(9):1726-37 doi 10.1210/me.2003-0031.
13. Lapuk AV, Wu C, Wyatt AW, McPherson A, McConeghy BJ, Brahmbhatt S*, et al.* From sequence to molecular pathology, and a mechanism driving the neuroendocrine phenotype in prostate cancer. J Pathol **2012**;227(3):286-97 doi 10.1002/path.4047.
14. Terry S, Beltran H. The many faces of neuroendocrine differentiation in prostate cancer progression. Front Oncol **2014**;4:60 doi 10.3389/fonc.2014.00060.

15. Kim J, Jin H, Zhao JC, Yang YA, Li Y, Yang X*, et al.* FOXA1 inhibits prostate cancer neuroendocrine differentiation. Oncogene **2017**;36(28):4072-80 doi 10.1038/onc.2017.50.
16. Li Y, Donmez N, Sahinalp C, Xie N, Wang Y, Xue H*, et al.* SRRM4 Drives Neuroendocrine Transdifferentiation of Prostate Adenocarcinoma Under Androgen Receptor Pathway Inhibition. Eur Urol **2016** doi 10.1016/j.eururo.2016.04.028.
17. Zou M, Toivanen R, Mitrofanova A, Floc'h N, Hayati S, Sun Y*, et al.* Transdifferentiation as a Mechanism of Treatment Resistance in a Mouse Model of Castration-resistant Prostate Cancer. Cancer discovery **2017** doi 10.1158/2159-8290.CD-16-1174.
18. Lee John K, Phillips John W, Smith Bryan A, Park Jung W, Stoyanova T, McCaffrey Erin F*, et al.* N-Myc Drives Neuroendocrine Prostate Cancer Initiated from Human Prostate Epithelial Cells. Cancer Cell **2016** doi 10.1016/j.ccell.2016.03.001.
19. Mu P, Zhang Z, Benelli M, Karthaus WR, Hoover E, Chen CC*, et al.* SOX2 promotes lineage plasticity and antiandrogen resistance in TP53- and RB1-deficient prostate cancer. Science **2017**;355(6320):84-8 doi 10.1126/science.aah4307.
20. Bishop JL, Thaper D, Vahid S, Davies A, Ketola K, Kuruma H*, et al.* The Master Neural Transcription Factor BRN2 is an Androgen Receptor Suppressed Driver of Neuroendocrine Differentiation in Prostate Cancer. Cancer discovery **2016** doi 10.1158/2159-8290.CD-15-1263.
21. Lin D, Wyatt AW, Xue H, Wang Y, Dong X, Haegert A*, et al.* High fidelity patient-derived xenografts for accelerating prostate cancer discovery and drug development. Cancer Res **2014**;74(4):1272-83 doi 10.1158/0008-5472.CAN-13-2921-T.
22. Akamatsu S, Wyatt AW, Lin D, Lysakowski S, Zhang F, Kim S*, et al.* The Placental Gene PEG10 Promotes Progression of Neuroendocrine Prostate Cancer. Cell reports **2015**;12(6):922-36 doi 10.1016/j.celrep.2015.07.012.
23. Beltran H, Rickman DS, Park K, Chae SS, Sboner A, MacDonald TY*, et al.* Molecular characterization of neuroendocrine prostate cancer and identification of new drug targets. Cancer discovery **2011**;1(6):487-95 doi 10.1158/2159-8290.CD-11-0130.
24. Grasso CS, Wu YM, Robinson DR, Cao X, Dhanasekaran SM, Khan AP*, et al.* The mutational landscape of lethal castration-resistant prostate cancer. Nature **2012**;487(7406):239-43 doi 10.1038/nature11125.
25. Kumar A, Coleman I, Morrissey C, Zhang X, True LD, Gulati R*, et al.* Substantial interindividual and limited intraindividual genomic diversity among tumors from men with metastatic prostate cancer. Nat Med **2016** doi 10.1038/nm.4053.
26. Cerami E, Gao J, Dogrusoz U, Gross BE, Sumer SO, Aksoy BA*, et al.* The cBio cancer genomics portal: an open platform for exploring multidimensional cancer genomics data. Cancer discovery **2012**;2(5):401-4 doi 10.1158/2159-8290.CD-12-0095.
27. Varambally S, Yu J, Laxman B, Rhodes DR, Mehra R, Tomlins SA*, et al.* Integrative genomic and proteomic analysis of prostate cancer reveals signatures of metastatic progression. Cancer Cell **2005**;8(5):393-406 doi 10.1016/j.ccr.2005.10.001.
28. Subramanian A, Tamayo P, Mootha VK, Mukherjee S, Ebert BL, Gillette MA*, et al.* Gene set enrichment analysis: a knowledge-based approach for interpreting

genome-wide expression profiles. Proc Natl Acad Sci U S A **2005**;102(43):15545-50 doi 10.1073/pnas.0506580102.

29. Liberzon A, Subramanian A, Pinchback R, Thorvaldsdottir H, Tamayo P, Mesirov JP. Molecular signatures database (MSigDB) 3.0. Bioinformatics **2011**;27(12):1739-40 doi 10.1093/bioinformatics/btr260.
30. Johnson BE, Whang-Peng J, Naylor SL, Zbar B, Brauch H, Lee E*, et al.* Retention of chromosome 3 in extrapulmonary small cell cancer shown by molecular and cytogenetic studies. J Natl Cancer Inst **1989**;81(16):1223-8.
31. Eissenberg JC, Elgin SC. HP1a: a structural chromosomal protein regulating transcription. Trends Genet **2014**;30(3):103-10 doi 10.1016/j.tig.2014.01.002.
32. Maison C, Almouzni G. HP1 and the dynamics of heterochromatin maintenance. Nature reviews Molecular cell biology **2004**;5(4):296-304 doi 10.1038/nrm1355.
33. Rickman DS, Beltran H, Demichelis F, Rubin MA. Biology and evolution of poorly differentiated neuroendocrine tumors. Nat Med **2017**;23(6):1-10 doi 10.1038/nm.4341.
34. Grewal SI, Jia S. Heterochromatin revisited. Nat Rev Genet **2007**;8(1):35-46 doi 10.1038/nrg2008.
35. Medvedeva YA, Lennartsson A, Ehsani R, Kulakovskiy IV, Vorontsov IE, Panahandeh P*, et al.* EpiFactors: a comprehensive database of human epigenetic factors and complexes. Database (Oxford) **2015**;2015:bav067 doi 10.1093/database/bav067.
36. Kleb B, Estecio MR, Zhang J, Tzelepi V, Chung W, Jelinek J*, et al.* Differentially methylated genes and androgen receptor re-expression in small cell prostate carcinomas. Epigenetics **2016**:0 doi 10.1080/15592294.2016.1146851.
37. Travis WD. Update on small cell carcinoma and its differentiation from squamous cell carcinoma and other non-small cell carcinomas. Mod Pathol **2012**;25 Suppl 1:S18-30 doi 10.1038/modpathol.2011.150.
38. De Koning L, Savignoni A, Boumendil C, Rehman H, Asselain B, Sastre-Garau X*, et al.* Heterochromatin protein 1alpha: a hallmark of cell proliferation relevant to clinical oncology. EMBO Mol Med **2009**;1(3):178-91 doi 10.1002/emmm.200900022.
39. Cheng W, Tian L, Wang B, Qi Y, Huang W, Li H*, et al.* Downregulation of HP1alpha suppresses proliferation of cholangiocarcinoma by restoring SFRP1 expression. Oncotarget **2016**;7(30):48107-19 doi 10.18632/oncotarget.10371.
40. Yu YH, Chiou GY, Huang PI, Lo WL, Wang CY, Lu KH*, et al.* Network biology of tumor stem-like cells identified a regulatory role of CBX5 in lung cancer. Scientific reports **2012**;2:584 doi 10.1038/srep00584.
41. Itsumi M, Shiota M, Yokomizo A, Kashiwagi E, Takeuchi A, Tatsugami K*, et al.* Human heterochromatin protein 1 isoforms regulate androgen receptor signaling in prostate cancer. Journal of molecular endocrinology **2013**;50(3):401-9.
42. Shapiro E, Huang H, Ruoff R, Lee P, Tanese N, Logan SK. The heterochromatin protein 1 family is regulated in prostate development and cancer. J Urol **2008**;179(6):2435-9 doi 10.1016/j.juro.2008.01.091.
43. Larson AG, Elnatan D, Keenen MM, Trnka MJ, Johnston JB, Burlingame AL*, et al.* Liquid droplet formation by HP1alpha suggests a role for phase separation in heterochromatin. Nature **2017** doi 10.1038/nature22822.

649 44. Nielsen AL, Ortiz JA, You J, Oulad-Abdelghani M, Khechumian R, Gansmuller A*, et*
650 *al.* Interaction with members of the heterochromatin protein 1 (HP1) family and
651 histone deacetylation are differentially involved in transcriptional silencing by
652 members of the TIF1 family. EMBO J **1999**;18(22):6385-95 doi
653 10.1093/emboj/18.22.6385.
654 45. Abe Y, Sako K, Takagaki K, Hirayama Y, Uchida KS, Herman JA*, et al.* HP1-Assisted
655 Aurora B Kinase Activity Prevents Chromosome Segregation Errors. Dev Cell
656 **2016**;36(5):487-97 doi 10.1016/j.devcel.2016.02.008.
657 46. Luijsterburg MS, Dinant C, Lans H, Stap J, Wiernasz E, Lagerwerf S*, et al.*
658 Heterochromatin protein 1 is recruited to various types of DNA damage. J Cell Biol
659 **2009**;185(4):577-86 doi 10.1083/jcb.200810035.
660 47. Lee YH, Kuo CY, Stark JM, Shih HM, Ann DK. HP1 promotes tumor suppressor
661 BRCA1 functions during the DNA damage response. Nucleic Acids Res
662 **2013**;41(11):5784-98 doi 10.1093/nar/gkt231.
663 48. Zhang W, Liu B, Wu W, Li L, Broom BM, Basourakos SM*, et al.* Targeting the MYCN-
664 PARP-DNA Damage Response Pathway inNeuroendocrine Prostate Cancer. Clin
665 Cancer Res **2017** doi 10.1158/1078-0432.CCR-17-1872.
666 49. Eissenberg JC, James TC, Foster-Hartnett DM, Hartnett T, Ngan V, Elgin SC.
667 Mutation in a heterochromatin-specific chromosomal protein is associated with
668 suppression of position-effect variegation in Drosophila melanogaster. Proc Natl
669 Acad Sci U S A **1990**;87(24):9923-7.
670 50. Yearim A, Gelfman S, Shayevitch R, Melcer S, Glaich O, Mallm JP*, et al.* HP1 is
671 involved in regulating the global impact of DNA methylation on alternative splicing.
672 Cell reports **2015**;10(7):1122-34 doi 10.1016/j.celrep.2015.01.038.

673

FIGURE LEGENDS

Figure 1. NEPC has a distinctive heterochromatin gene signature. (A-F) GSEA show the enrichment of heterochromatin-associated genes in NEPC from (A) PDX models, (B) the *Beltran et al.* 2011 cohort (23), (C) the *Beltran et al.* 2016 cohort (10), and in NE-like GEM models derived from (D) *Rb/Tp53* DKO or *Pten/Rb/Tp53* TKO (11), (E) *NPp53* CRPC with NE differentiation (17), (F) and *Nmyc* overexpression (8). “NES” stands for normalized enrichment score; FDR q values were calculated using 1000 gene permutations except for (C), where Gsea preranked was applied. (G) Heatmap showing the hierarchical clustering among all PDX samples suggests a unique upregulation of heterochromatin signature genes in NEPC PDX tumors. (H) Weighted NE scores and heterochromatin scores of adenocarcinoma and NEPC PDX tumors and two clinical cohorts. NE scores were calculated based on the gene panels from *Beltran et al.* 2016 (10) and *Lee et al.* 2016 (18). Heterochromatin scores were calculated based on the weighted gene panel from (G). Scatter plots show the calculated score of each tumor sample, with lines indicating the mean value and 95% CI. The *p*-values were calculated using the unpaired two-tail Student’s *t*-test. See also Fig. S1.

Figure 2. HP1α expression is upregulated during NE transdifferentiation and in NEPC PDX models. (A) A heatmap showing the gene expression changes in the LTL331/331R NE transdifferentiation PDX model. Heterochromatin signature genes, AR signaling targets, and NE markers are included. RNA-seq data from two individual samples at each time point was used (pre: LTL331 pre-castration; Cx: 8 weeks post-castration; Rep: LTL331R NEPC

relapse). Average differences in expression between castrated and pre-castrated tumors (C vs. P) are shown in a separate heatmap. (B-D) HP1α expression in PDX models, as determined by (B) qRT-PCR, (C) IHC, and (D) Western blotting. Scatter plots show relative mRNA expression or IHC score for each sample, with lines indicating median values. (E-G) HP1α expression in the LTL331/331R castration-induced NE transdifferentiation PDX model, as determined by (E) qRT-PCR, (F) Western blotting, and (G) IHC. Data show mean ± SEM from three replicates. The *p*-values (B, C, E) were calculated with unpaired two-tail Student's *t*-tests. See also Fig. S2.

Figure 3. HP1α expression is upregulated in clinical NEPC samples and correlates with poor prognosis in adenocarcinomas. (A-C) *HP1α* mRNA expression in NEPC vs. adenocarcinoma from (A) the *Beltran, et al.* 2011 cohort (23), (B) the *Beltran, et al.* 2016 cohort (10), and (C) the *Grasso, et al.* 2012 cohort (24). Scatter plots show RNA expression data of each sample, with lines indicating median values. The *p*-values were calculated using unpaired two-tail Student's *t*-test. (D) Staining intensity for the HP1α protein in primary adenocarcinomas (n=103), CRPC-adenocarcinomas (n=120), and NEPC (n=8) as determined by IHC of the VPC TMA. Box plots show the mean with whiskers representing 5-95% percentile values. The *p*-values were calculated using unpaired two-tail Student's *t*-test. (E) Representative IHC images for the various staining intensities (0 to 3) are shown, with the lower panels being magnifications of the selected regions in the upper panels. Scale bars in the upper and lower panels represent 100 μm and 10 μm respectively. (F-G) Kaplan-Meier survival analyses of estimated (F) relapse-free survival time based on the HP1α IHC score of primary adenocarcinomas from the VPC cohort with follow-up information (n=37)

and (G) prostate-cancer specific survival time after first hormonal therapy based on *HP1α* mRNA from metastatic adenocarcinomas in the *Grasso, et al.* 2012 cohort (n=33) (24). The *p*-values were calculated using the log-rank test to determine the difference in outcomes between patients with high (red) and low (black) *HP1α* expression.

Figure 4. HP1α is essential for the aggressive growth of NEPC cells and tumors. (A) Stable knockdown of *HP1α* in NCI-H660 cells by lentiviral transduction. Changes to *HP1α* mRNA and protein levels were determined by qRT-PCR and Western blotting respectively. Bar graph shows mean ± SEM. The *p*-value was calculated by unpaired two-tail Student's *t*-test. (B) Cell growth assay of *HP1α* knockdown H660 cells as determined by crystal violet staining. Stable cells were plated in four replicate wells for each time point and cell numbers were determined based on the absorbance at O.D. 572 nm of crystal violet dissolved in 2% SDS. Data is graphed as mean ± SEM. Representative images demonstrating cell numbers at the final time point are shown. The *p*-value was calculated by two-way ANOVA. (C) Colony formation assay of *HP1α* knockdown H660 cells as determined by crystal violet staining. Cells were plated in four replicate wells for each stable line and colony numbers were counted manually. Bar graph shows mean ± SEM. Representative images demonstrating colony numbers are shown. The *p*-value was calculated by unpaired two-tail Student's *t*-test. (D) An EdU incorporation assay was performed by incubating stable *HP1α* knockdown H660 cells with 10 μM EdU for 4 hours. EdU-labeled cells (red) and total cells counterstained with DAPI (blue) were counted for at least 10 fields. Bar graph shows the mean (EdU-positive ratio) ± SEM. Representative images are shown with the scale bar representing 100μm. The *p*-values were calculated by unpaired two-tail Student's *t*-test. (E)

739 An apoptosis assay measuring caspase-3 activity using the ApoLive-Glo™ Multiplex
740 Reagent. Relative apoptosis was determined by the ratio of luminescence (caspase-3
741 activity) to fluorescence (AFC signal for viable cells). Bar graph shows mean ± SEM
742 (normalized to shC). The *p*-values were calculated by unpaired two-tail Student's *t*-test. (F)
743 Cell death following stable *HP1α* knockdown in H660 cells was determined by flow
744 cytometry with 7-AAD staining. 10,000 single cells were collected for analysis with dead cells
745 being 7-AAD positive. Bar graph shows mean ± SEM (normalized to shC). The *p*-values
746 were calculated by unpaired two-tail Student's *t*-test. (G) Apoptosis markers cleaved-
747 caspase 3 and cleaved-PARP1 as determined by Western blotting following stable *HP1α*
748 knockdown in H660 cells. Intact caspase 3 and PARP1 serve as controls. Cl stands for
749 "cleaved". (H) Selected gene sets enriched in *HP1α*- versus *control*- knockdown H660 cells
750 as analyzed by GSEA. The x-axis represents normalized enrichment score (NES). FDR of all
751 gene sets is less than 0.05 calculated by 1000 permutations. (I-J) Stable H660 cell lines shC
752 and KD2 were each grafted into four NSG mice (eight tumors total) to assess *in vivo*
753 xenograft tumor growth. (I) Tumor volume was measured starting from when palpable tumor
754 appears to when mice were euthanized. Line graph shows mean ± SEM, with *p*-value
755 calculated by two-way ANOVA. Tumor images are shown in the right panel. (J) Fresh tumors
756 were also weighed at sample collection. Bar graph shows mean ± SEM with The *p*-value
757 was calculated by unpaired two-tail Student's *t*-test. See also Fig. S3.

758 **Figure 5. HP1α promotes NE transdifferentiation of prostatic adenocarcinoma cells**
759 **following ADT.** (A) Ectopic expression of *HP1α* in LNCaP-V16D cells as determined by
760 Western blotting. (B-C) Induction of NE transdifferentiation with ADT in V16D cells stably

761 overexpressing *HP1α*. Relative mRNA and protein expression of terminal NE markers (SYP,
762 CHGA, NSE, NCAM1) were detected by (B) qRT-PCR and (C) Western blotting in stable
763 cells cultured in complete medium (FBS), CSS, and CSS with 10 μM EnZ 14 days. Bar
764 graphs show mean ± SEM. The *p*-values were calculated by unpaired two-tail Student's *t*-
765 tests comparing *HP1α- to control- overexpressing cells*. Relative band intensities as
766 determined by ImageJ are indicated, with actin serving as internal control. (D) A heatmap
767 comparing expression of NEPC marker genes in the indicated V16D cells upon EnZ
768 treatment. The select NEPC marker genes upregulated by *HP1α* overexpression are
769 similarly upregulated in clinical NEPCs in the *Beltran, et al.* 2011 cohort (23). (E) Top 10
770 pathways significantly enriched in *HP1α* overexpressing V16D cells compared to control
771 cells as analyzed with IPA. (F-G) Pearson correlation analysis of *HP1α* mRNA expression
772 and the expression of various NE markers in advanced PCa samples. (F) Correlation with
773 *NCAM1* and *NSE* expression in the *Beltran, et al.* 2016 cohort (10), and (G) correlation with
774 *CHGB* and *CHGA expression* in the *Kumar et al.* 2015 cohort (25). See also Fig. S4.

775 **Figure 6. HP1α represses AR and REST expression and enriches H3K9me3 on their**
776 **promoters.** (A-B) AR and REST expression in stable V16D cells overexpressing *HP1α* as
777 determined by (A) qRT-PCR and (B) Western blotting. Bar graphs show mean ± SEM. The
778 *p*-values were calculated by unpaired two-tail Student's *t*-test. (C) A heatmap comparing
779 expression of AR signaling genes in the indicated V16D cells. The select AR target genes
780 downregulated by HP1α overexpression are similarly downregulated in clinical NEPCs in the
781 Beltran, et al. 2011 cohort (23). (D) GSEA of V16D cells with stable *HP1α* overexpression.
782 Expression of pericentric heterochromatin components are upregulated by *HP1α*

overexpression. “NES” stands for normalized enrichment score; FDR q values were calculated using 1000 gene permutations. (E) ChIP-PCR shows the enrichment of H3K9me3 on the promoters of *AR* and *REST* in V16D cells with *HP1α* overexpression, *NC* is a negative control region. Bar graphs show mean ± SEM. The *p*-values were calculated by unpaired two-tail Student’s *t*-test. (F) GSEA show the enrichment of pericentric heterochromatin genes in human NEPC samples and mouse NE-like tumors. The y-axis represents normalized enrichment score (NES) and the x-axis denotes clinical cohorts and GEM models. FDR is less than 0.15 calculated by 1000 permutations. (G-H) Pearson correlation analysis of *HP1α* mRNA expression and *AR* and *REST* mRNA levels from (G) the *Beltran et al.* 2016 (10) and (H) the *Kumar et al*. 2016 cohorts (25). See also Fig. S5.

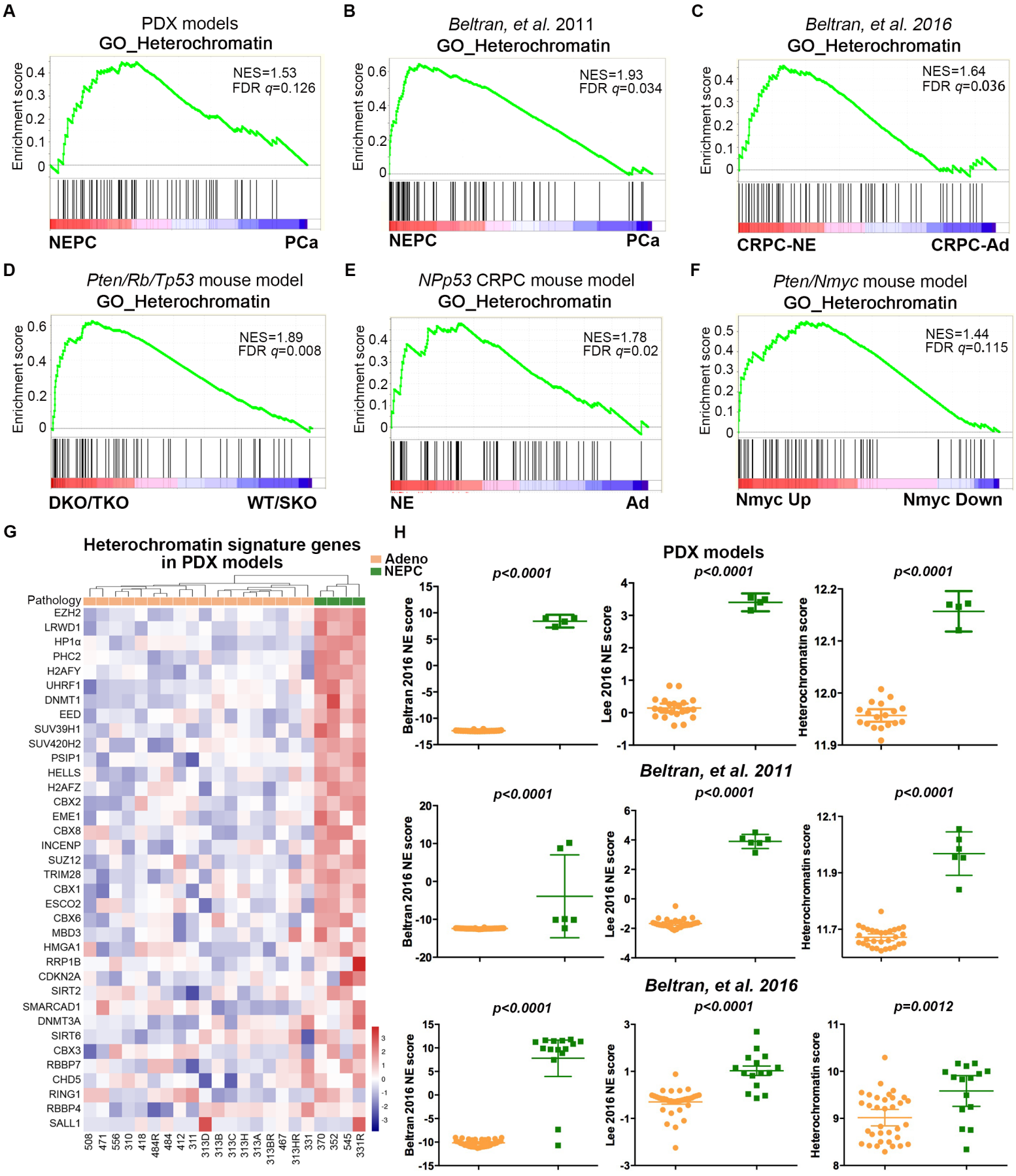

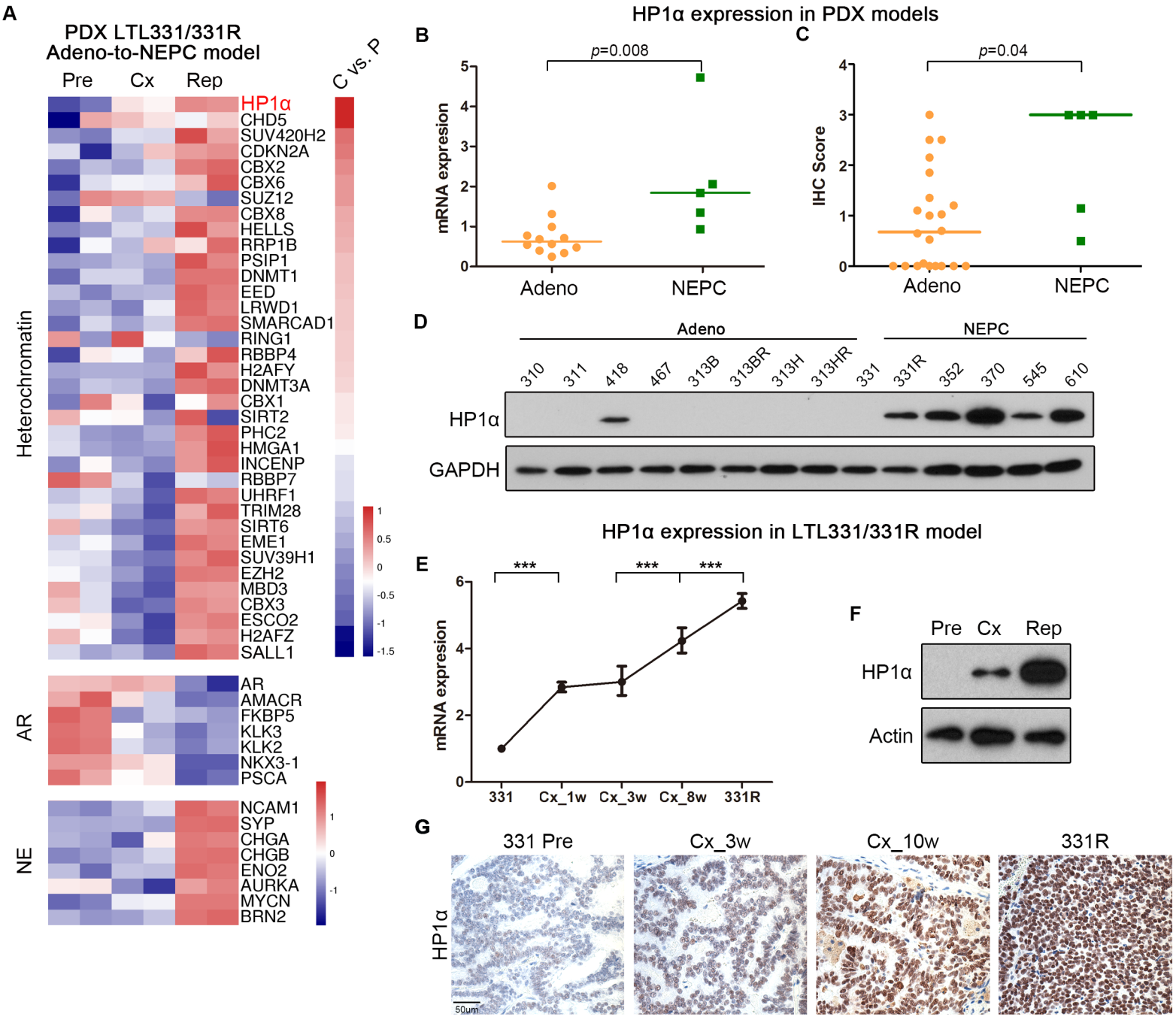

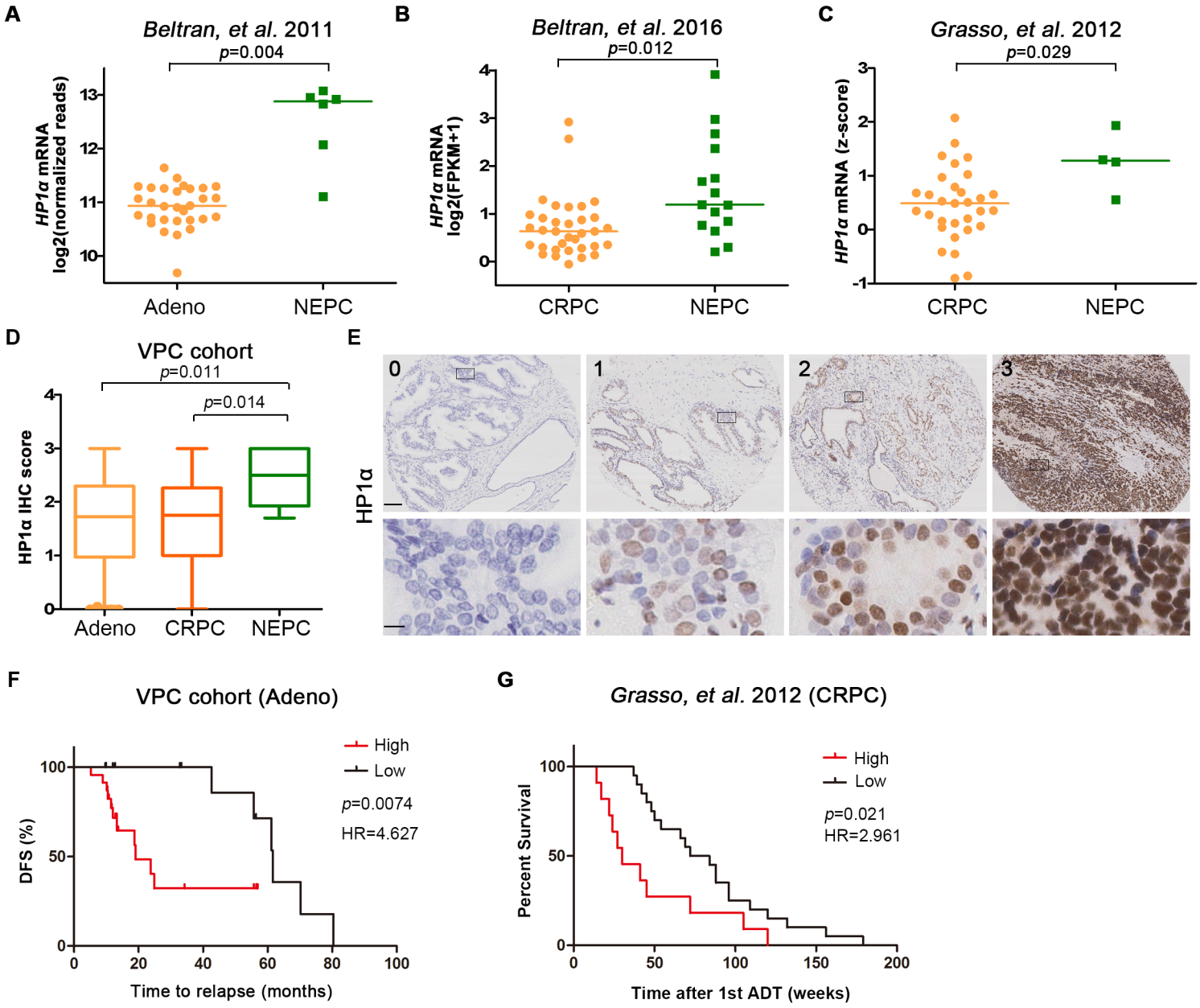

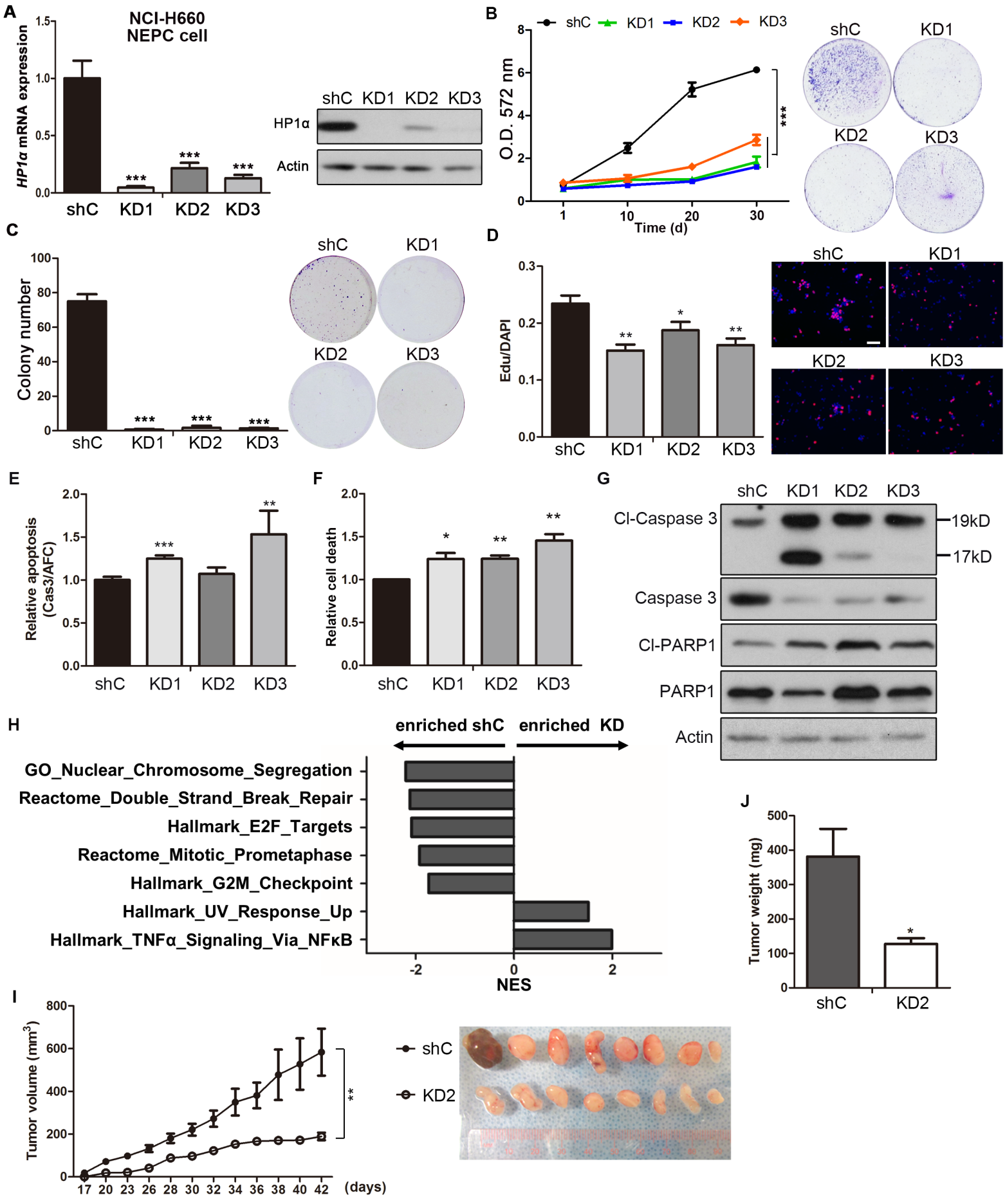

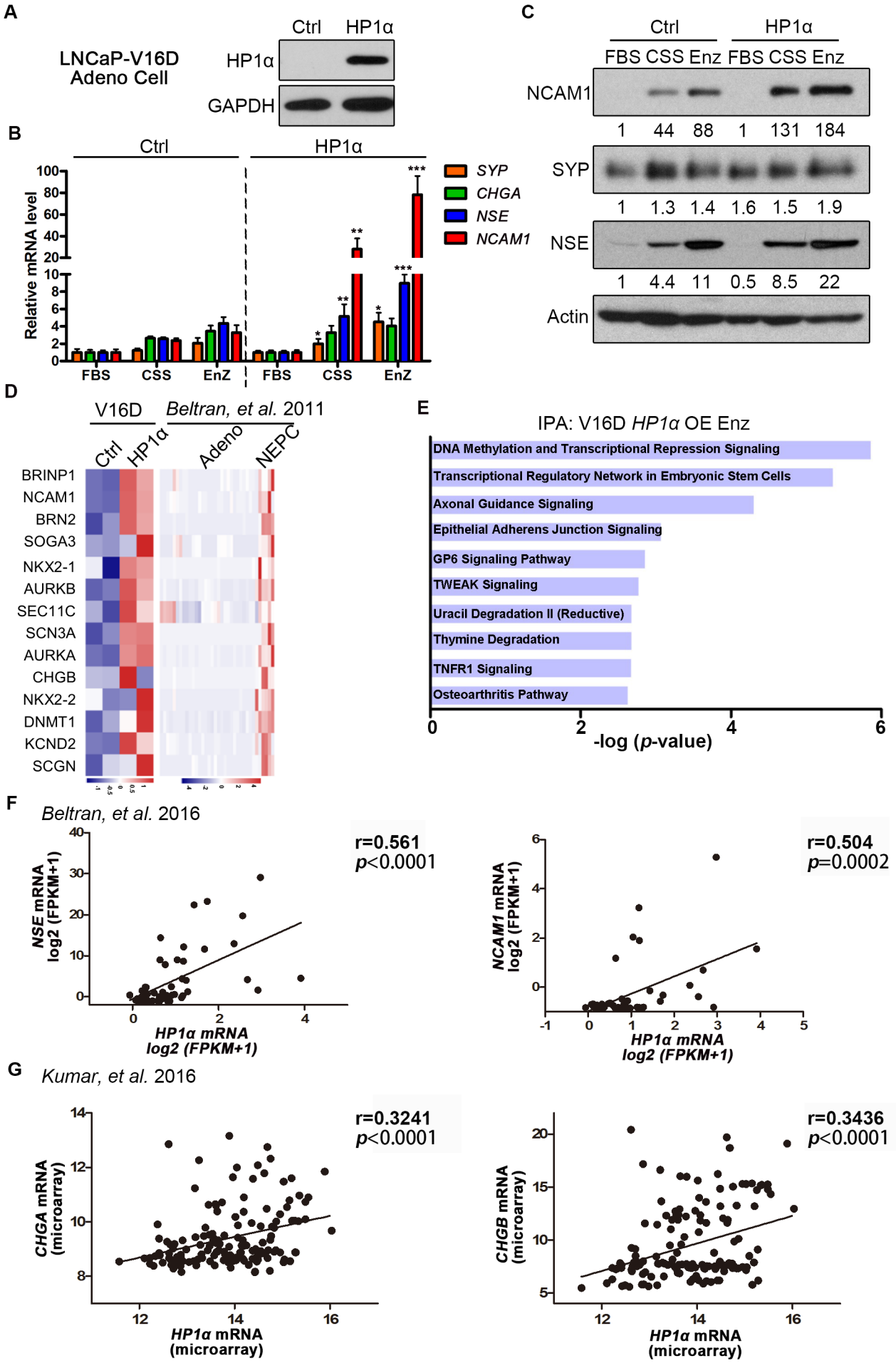

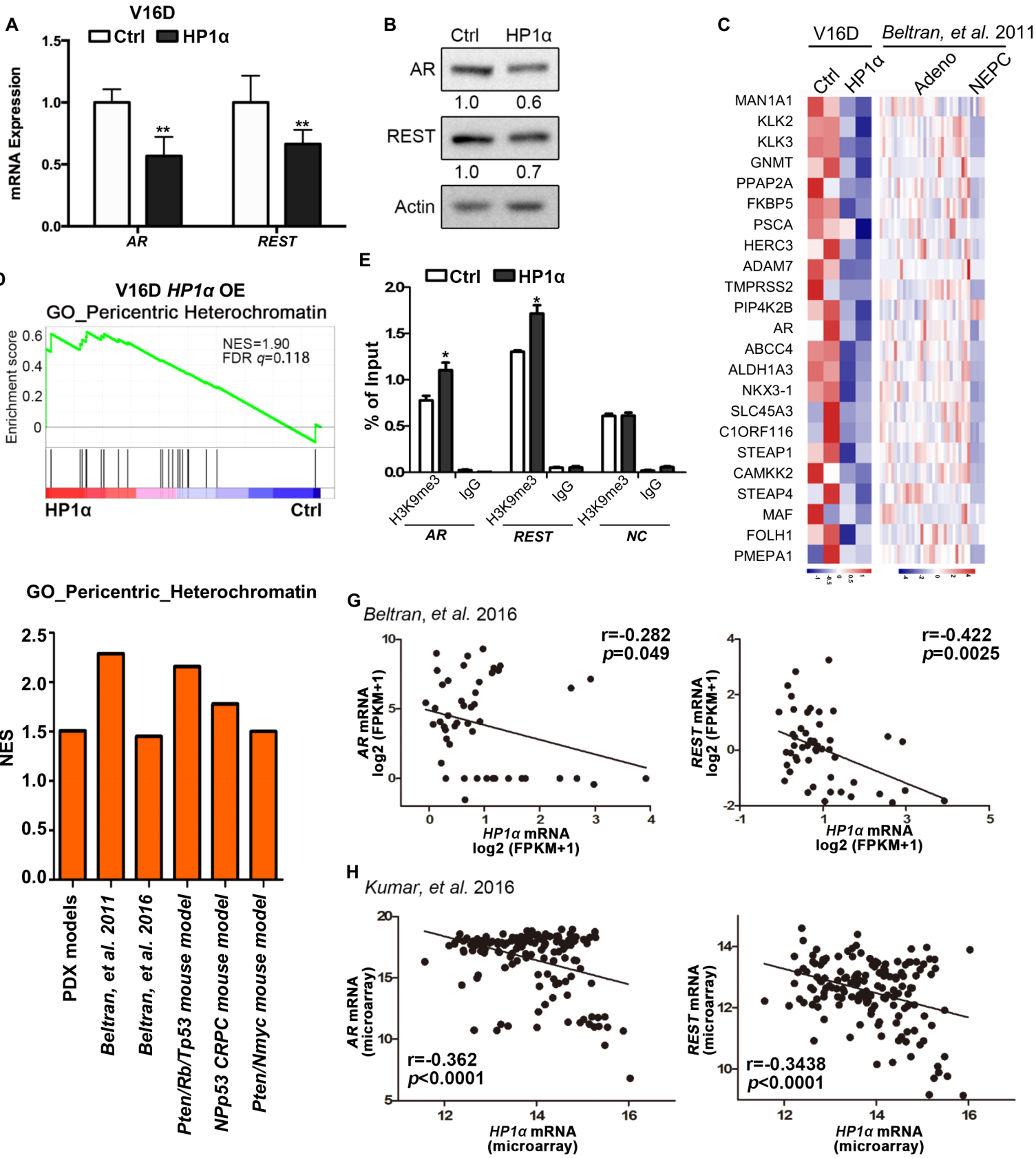

AACR American Association for Cancer Research

Cancer Research

The Journal of Cancer Research (1916–1930) | The American Journal of Cancer (1931–1940)

Heterochromatin protein 1α mediates development and aggressiveness of neuroendocrine prostate cancer

Xinpei Ci, Jun Hao, Xin Dong, et al.

Cancer Res Published OnlineFirst February 27, 2018.